Ostrich 2021: 1–9
Printed in South Africa — All rights reserved
This is the final version of the article that is
published ahead of the print and online issue

OSTRICH
ISSN 0030–6525 EISSN 1727-947X
https://doi.org/10.2989/00306525.2021.1995908

Investigating the influence of the extreme Indian Ocean Dipole on the 2020 influx of Red-necked Phalaropes *Phalaropus lobatus* in Kenya

Raphaël Nussbaumer[1,2]*, Mathieu Gravey[3], Améline Nussbaumer[1] and Colin Jackson[1]

[1] *A Rocha Kenya, Watamu, Kenya*
[2] *Swiss Ornithological Institute, Sempach, Switzerland*
[3] *Institute of Earth Surface Dynamics, University of Lausanne, Lausanne, Switzerland*
**Correspondence: raphael.nussbaumer@arocha.org*

Ocean currents have wide-ranging impacts on seabird movement and survival. By extension, the extreme oscillations they are subject to, such as extreme Indian Ocean Dipole (IOD) events, can also be expected to dramatically influence seabird populations. This study links the extreme IOD event that occurred in 2019–2020 to the unusually high number of Red-necked Phalarope sightings observed in February 2020. We show that the extreme IOD event resulted in low net primary productivity (a measure of plankton growth) offshore from the Somalia-Kenyan coast, where Phalaropes have been tracked in previous winters. We suggest that Phalaropes were therefore forced to move closer to the coast to find food at river estuaries, thus explaining the influx in February 2020. This study calls for closer monitoring of seabird populations in East Africa, particularly during extreme IOD events, which are expected to become more common in the future.

L'influence de l'oscillation extrême du Dipôle de l'Océan Indien sur l'afflux de Phalaropes à bec étroit *Phalaropus lobatus* au Kenya en 2020

Les courants océaniques exercent une forte influence sur les déplacements et la survie des oiseaux marins. Par extension, on peut s'attendre à ce que les oscillations extrêmes auxquelles ces courants sont soumis, telles que les phases extrêmes du Dipôle de l'Océan Indien (DOI), aient une influence d'autant plus forte sur les populations d'oiseaux marins. Cette étude établit un lien entre l'oscillation extrême de DOI en 2019–2020 et le nombre exceptionnellement élevé de Phalaropes à bec étroit observé sur la côte kenyane en février 2020. Nous démontrons que ce DOI extrême a entraîné de faibles taux de production primaire nette (une mesure de la croissance du plancton) au large des côtes somaliennes et kenyanes, où des Phalaropes avaient été suivies au cours des hivers précédents. Nous suggérons que les Phalaropes ont par conséquent été contraintes de se rapprocher de la côte pour se nourrir dans les estuaires des rivières, expliquant ainsi l'afflux observé en février 2020. Cette étude appelle à une surveillance plus étroite des populations d'oiseaux marins en Afrique de l'Est, en particulier lors d'oscillations extrêmes de DOI, qui ne devraient que s'accentuer à l'avenir.

Keywords: birds, currents, East Africa, Kenya, migration, ocean, primary productivity, seabirds, upwelling, wintering

Introduction

Ocean currents have a profound impact on the distribution and abundance of marine wildlife and, at the top of the food chain, on seabirds (e.g. Pocklington 1979). Through the process of upwelling (redistributing nutrients from deeper ocean layers to the surface (e.g. Franks 1992), currents influence the spatio-temporal distribution of plankton, and, by extension, marine wildlife as a whole (e.g. Hunt et al. 1999; Bost et al. 2009). These currents usually follow predictable patterns on a large scale (Bjerknes 1969), upon which much of the marine wildlife rely to find nutrient-rich waters (e.g. Weimerskirch 2007). However, currents can be subject to annual variation, due to naturally occurring ocean-atmosphere oscillations, such as the *El Niño* Southern Oscillation (ENSO) in the Pacific Ocean.

In the Indian Ocean, the main source of interannual variability is the Indian Ocean Dipole (IOD), also known as the Indian Niño (Saji et al. 1999; Webster et al. 1999). Similar to the ENSO, the IOD is characterised by warm and cool phases occurring irregularly every few years and affecting the general distribution of planktonic food in the Indian Ocean (Wiggert et al. 2009). The IOD has been shown to impact temperature and precipitation in continental East Africa (Behera et al. 2005), with wide-ranging ripple effects on biodiversity (Marchant et al. 2007) and the human economy. IOD magnitude has been shown to be correlated with seabird abundance (Perez-Correa et al. 2020) and breeding success (Monticelli et al. 2007; Rivalan et al. 2010). The IOD was also shown to influence stopover conditions for Palearctic landbird migrants (Hušek et al. 2009; Tøttrup et al. 2012; Tryjanowski et al. 2013; Tobolka et al. 2018; Remisiewicz and Underhill 2020).

As regular IODs are known to influence seabirds, a fortiori, extreme IOD events can be expected to have

Published online 07 Dec 2021

dramatic effects on seabird populations through their proven impact on fisheries, such as in 1997–1998 (Marsac and Blanc 1999; Jacobs et al. 2020b, Jebri et al. 2020). Indeed, the equivalent phenomenon of *El Niño* in the Pacific Ocean has been shown to affect the reproductive success of seabirds during the extreme event of 1982–1983 (Barber and Chavez 1983; Ainley et al. 1988).

In this paper, we link the exceptionally high number of Red-necked Phalaropes *Phalaropus lobatus* observed along the Kenyan coast in February 2020 to the concurrent extreme positive Indian Ocean Dipole (IOD) of 2019/2020.

Materials and methods

Studied area: coastal upwelling and IOD in East Africa

Along the coast of Africa, the location and magnitude of upwelling is governed by the Indian Monsoon Current (Painter 2020), a complex and seasonally variable phenomenon, the causes and effects of which are still being researched today (see reviews by Schott et al. 2009; Vinayachandran et al. 2021). More specifically, upwelling occurs during the northeast monsoon (November to April) at the convergence zone of the northward flowing East African Coastal Current and the southward flowing Somali Current (Figure 1a). Due to Ekman transport, it then moves eastwards away from the coast (Heip et al. 1995; Lévy et al. 2007; Vinayachandran et al. 2021) (Figure 1a). Directly off the northern coast of Kenya, upwelling is further strengthened by topographically induced shelf-break upwelling (Jacobs et al. 2020a) (Figure 1a).

Studied species: Red-necked Phalaropes in East Africa

In East Africa, Red-necked Phalaropes sighted are part of a Palearctic population wintering in the Arabian Sea, mainly in the Gulf of Aden (Bailey 1966; Rubega et al. 2020). They are considered a common winter visitor on the North East coast of Somalia and present in large numbers along the entire coast (Bailey 1971; Schiemann 1986; Ash and Miskell 1998; Delany et al. 2009). In Kenya, Red-necked Phalaropes are present from October to March (Britton and Britton 1979) with counts of hundreds described as regular on the coast (Britton 1980; Lewis and Pomeroy 1989). More specifically, they have been reported at locations where sea-surface temperatures indicate upwelling (Bailey 1971), corresponding to the edge of the coastal shelf at the intersection of the Somali and the East African coastal currents (Schiemann 1986).

Recent geolocator studies (Van Bemmelen et al. 2016, 2019) provided further insight into the Red-necked Phalaropes' wintering movements and their drivers. Van Bemmelen et al. (2019) suggest that Red-necked Phalaropes of the Palearctic population travel long distances during their non-breeding periods, a strategy called itinerancy (Moreau 1972), in order to follow the predictable seasonal and spatial variation of the oceanic net primary productivity (NPP). Their study showed Red-necked Phalaropes travelling as far south as the Kenyan coast in the second part of their winter (January–March).

Sightings in 2020

The sightings of Red-necked Phalaropes collected in February 2020 were either opportunistic sightings or part of the regular waterbird counts performed by the A Rocha Kenya Science team (Nussbaumer et al. 2020). For all sightings, we recorded the date, location, count size and moulting when possible. Identification was either made by experienced birdwatchers on the field or based on pictures shared by local anglers or tourists.

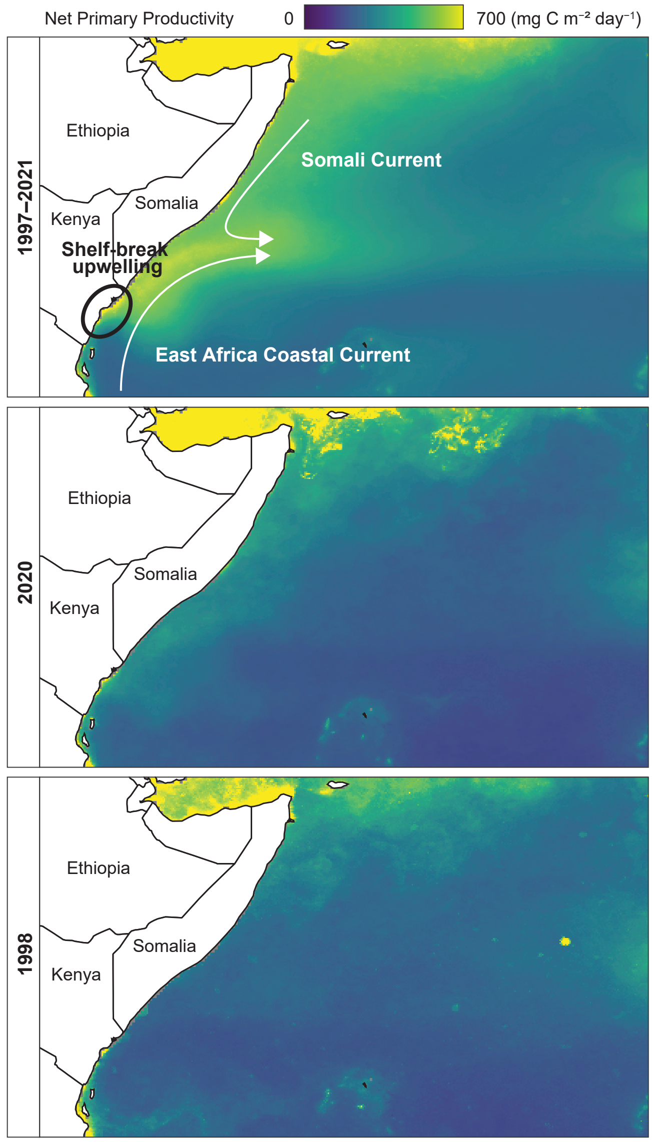

Figure 1: Map of Net Primary Productivity (NPP) averaged for January–March on the western Indian Ocean

Historical sightings

To assess the occurrence and wintering movements of Red-necked Phalaropes in the Indian Ocean and provide context for the 2020 sightings, we performed an exhaustive search of all previous records for this species across East Africa (Ethiopia, Kenya, Tanzania, Uganda), including sightings recorded in literature (East African Bird Report, Scopus, African Bird Club Bulletin) and on citizen science databases (EBird 2020; Kenya Bird Map 2020) (see data accessibility statement). We draw out seasonal and spatial patterns in terms of both number of sightings and count size. The spatial analysis was performed by grouping sightings made inland and on the coast.

Net Primary Productivity, Dipole Mode Index and number of sightings

During the boreal autumn of 2019, an unprecedented positive IOD took place (Lu and Ren 2020; Shi and Wang 2021), causing the absence of upwelling in the western Indian Ocean in January–March (Shi and Wang 2021). We analysed net primary productivity (NPP) data from remote satellite imagery to assess food availability during the months of January to March, which correspond to the period where Red-necked Phalaropes are most present on the coast. We compared the NPP maps of 2019–2020 and 1997–1998, both corresponding to extreme IOD events, with the average NPP data for all years available (1998–2021). The NPP data were computed using the Vertically Generalised Production Model (VGPM) algorithm (Behrenfeld and Falkowski 1997) retrieved from http://sites.science.oregonstate.edu/ocean.productivity (O'Malley 2020) and analysed with Google Earth Engine (Gorelick et al. 2017). We developed an interactive web map comparing the average NPP over several years for the months of interest.

We extracted the average NPP between October and March for each year over the area covering the convergence zone between the Somalia and East African coastal currents (Figure 1). Because NPP from satellite data is only available since 1997, we downloaded timeseries of the Dipole Model Index (DMI), a proxy measuring the intensity of IOD based on the gradient of sea-surface temperature, from https://psl.noaa.gov/gcos_wgsp/Timeseries/DMI. We computed the average DMI for the eastern Indian Ocean between October and March of each year since 1960. Finally, we explored the relationship between the yearly NPP, DMI and number of sightings on the coast with a linear regression between NPP and DMI

$NPP_y \sim DMI_y$ and a generalised linear regression with a Poisson family between the number of sightings and DMI, including year as a covariate,

$$\#sightings_y \sim Poisson(\mu_y)$$
$$log(\mu_y) = DMI_y + year_y$$

where $\#sightings_y$ is the number of RNP observed during year y.

Results

2020 sightings

As compared with usual sightings at this time of year, an exceptionally high number of Red-necked Phalaropes was observed along the Kenyan coast in February 2020, both in terms of group size and occurrence.

The most noteworthy sighting was recorded on 9 February 2020, at the Kongo river mouth (4°15′40″ S, 39°36′40″ E; Diani, Kenya). Several large flocks of small waders were observed flying and landing on the water offshore beyond the coral reef at approximately 07:00. To confirm this sighting, we hired a small fishing boat and identified the waders as Red-necked Phalaropes between 2 and 3 km offshore from Diani Beach, Mombasa (Figure 2). The Phalaropes' movements and the small boat we were in rendered it difficult to make more precise counts. A total estimate of 3 000 (2 000–5 000) individuals was made by the three observers, based on the encounter of five to seven large groups (100–600 birds in each), as well as multiple smaller groups (<100 birds). The individuals observed showed a suspended moult, similar to the dead bird found by Britton and Britton (Britton and Britton 1979). More pictures are available at https://github.com/A-Rocha-Kenya/Red-Necked-Phalaropes-in-East-Africa/tree/main/Media.

During the same month, Red-necked Phalaropes were also sighted at the following locations along the coast: Tana River Delta (single bird.14.02.2020), Mida Creek (single, 17.02.2020), Temple Point, Watamu (single, 22.02.2020), Watamu Beach (single, 23.02.2020) and a small vlei inland of Plot 37, Watamu, subsequently known as 'Phalarope Vlei' (two birds, 24–26.02.2020) (Nussbaumer et al. 2021). Furthermore, sports fishermen in Watamu who daily spend the whole day several kilometers offshore reported 'huge numbers' of Phalaropes in 2020 (P Darnborough, local fisher, pers. comm.).

Historical sightings

Drawing together all past sightings (n = 105; 1962–2020), our analysis suggests that Red-necked Phalaropes are present in East Africa from September to May, with a first peak from mid-October to early December and a second peak from mid-January to end of February (Figure 3). During the first peak, most sightings are recorded inland (34 vs 6 on the coast) and in low numbers (mean of 3.5 individuals), suggesting a potential overshooting of post-breeding migratory birds. During the second peak, Red-necked Phalaropes are slightly more common on the coast (31 vs 30 inland) and in higher numbers (mean of 33), potentially describing a population wintering off the coast of Kenya. Note that the count of 3 000 presented in this paper is not included in this analysis. Coastal records include 20 records offshore (i.e. on and beyond the fringing coral reef) (mean of 47 ind.), seven records onshore (mostly single birds), and eight records on saltworks (mean of eight individuals), which constitute prime habitat for food (e.g. Baker 2013). We only found three records of >one hundred birds (46% of all sightings are of single individuals and 78% are of less than 10 individuals). Records of smaller numbers inland (average of 4.6 ind.), mainly at the large lakes along the Great Rift Valley (Ethiopia, Uganda, Kenya and Tanzania) indicate an inland movement (Ash and Ashford 1977; Urban et al. 1986; Delany et al. 2009).

Net Primary Productivity, Dipole Model Index and sightings

The NPP maps confirm that in usual years (average for the period 1997–2021, Figure 1a), a bloom is visible offshore of the Kenyan-Somalian border, both at the shelf-break upwelling and at a larger scale where the East African Coastal Current meets the Somali Current. However, during years with a strong positive IOD (1998 and 2020), this bloom is completely absent (Figures 1b to 1c). A comparative map of NPP for each year is available at https://rafnuss.users.earthengine.app/view/net-primary-productivity.

The Dipole Model Index (DMI) in the western Indian Ocean is negatively correlated (−0.70) with the average

Figure 2: A small group of the large numbers of Red-necked Phalaropes recorded 2 km offshore on 9 February 2020. A total of 3 000 individuals was estimated, split into 5–7 large groups (100–600 each), and several smaller groups (<100)

NUMBER OF INDIVIDUALS

Mean (min–max; *n* = size)	Jan–May	Sep–Dec
Inland	5.9 (1–39; *n* = 30)	3.5 (1–40; *n* = 34)
Coast	32.7 (2–200; *n* = 31)	14.3 (1–50; *n* = 6)
Onshore	8.4 (1–28; *n* = 8)	
Offshore	1.1 (1–2; *n* = 7)	
Saltwork	47.1 (1–200; *n* = 20)	

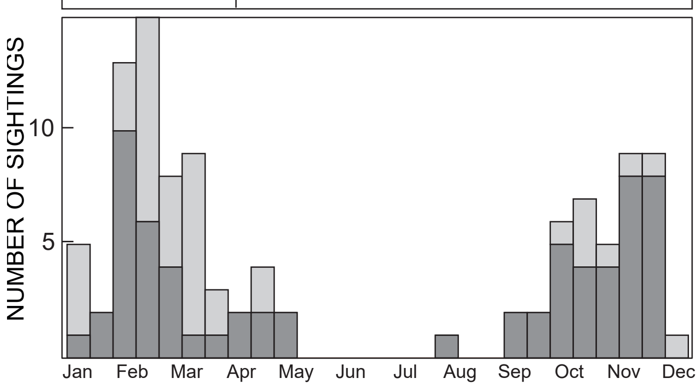

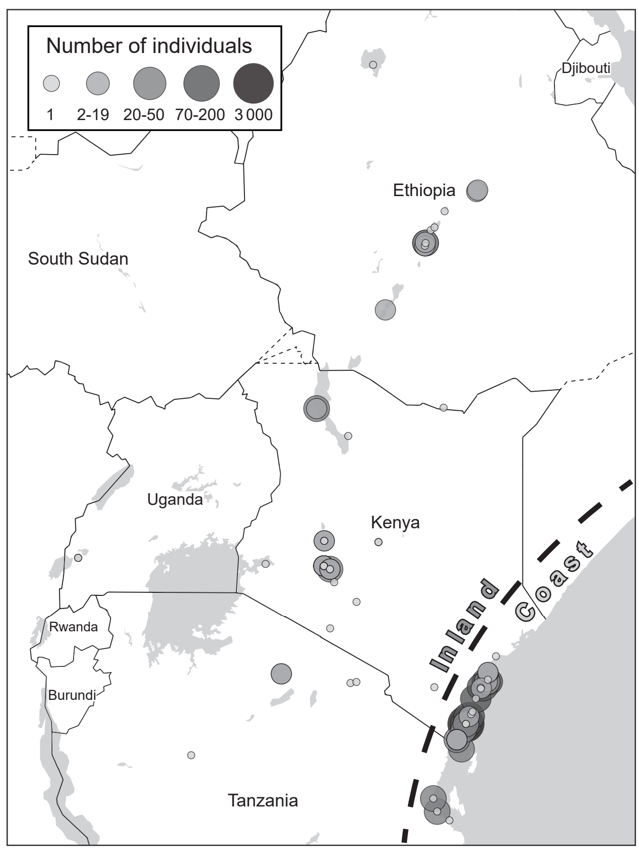

Figure 3: Summary of the 105 sightings in East Africa (Ethiopia, Uganda, Tanzania, and Kenya) found in the literature and citizen science platform ranging from 1962 to 2020

NPP of the area covering the possible East African wintering site of Red-necked Phalaropes offshore of Somalia (Figure 4). However, this linear relationship (Table A1 in Appendix A) shows significant variability (R^2 = 0.47) indicating that the amount of food available (i.e. NPP) may also depend on other local-scale effects. Between 1998 and 2020, the number of sightings is poorly related to the NPP (R^2 = 0.06), most notably with the absence of observations in 1998.

We extend the analysis of the influence of the IOD on observations of Red-necked Phalaropes on the coast to 1960–2020 by using DMI timeseries (Figure A1 in Appendix A). The number of sightings shows a weak positive relationship with the DMI (Figure 5), as well as a weak positive temporal trend (Figure A1 and Table A1 in Appendix A). This relationship is potentially spurious as we also note an increase in the DMI, due to greenhouse gas emissions (e.g. Cai et al. 2013), as well as enhanced observation pressure (number of observers, equipment, citizen science and improvement in data collection). Furthermore, the model fit is highly sensitive to the 2019 data point.

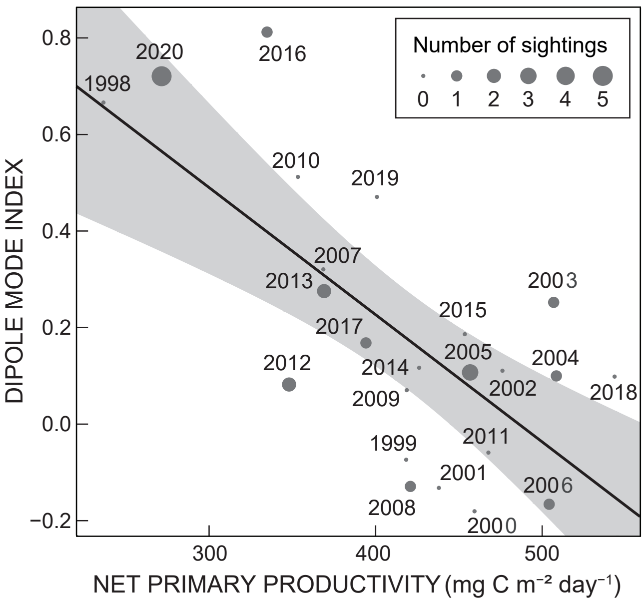

Figure 4: Scatter plot of the average DMI and NPP (October–March) and total number of sightings on the coast between 1998 and 2020. The fitted linear regression is shown with an black line and its corresponding uncertainty (95% confidence interval) as grey area

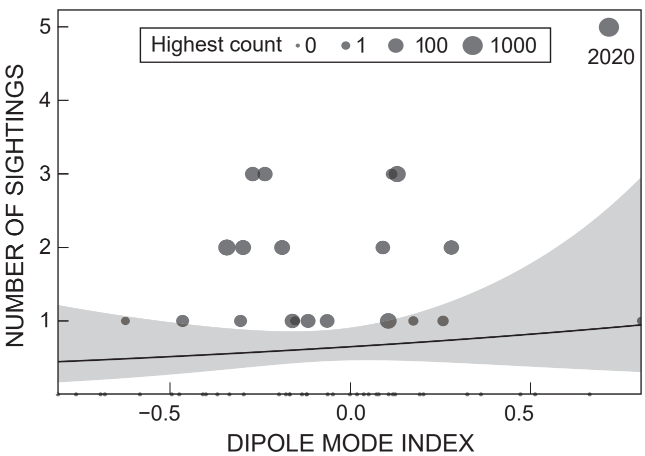

Figure 5: Number of times Red-necked Phalaropes were observed on the coast for each wintering period (October–March) based on the average Dipole Model Index for the same period on the western Indian Ocean. The highest count seen during this period is illustrated by the size of the dots (log-scale). The partial plot of the fitted generalized linear model is illustrated with the black line and corresponding uncertainty (grey area)

Discussion

Red-necked Phalaropes winter off the coast of East Africa

Relatively little is known about wintering Red-necked Phalaropes on the East African coast, to such an extent that this region does not feature on distribution maps for the species (BirdLife International 2020; Rubega et al. 2020). Yet, observations inland and of large numbers offshore (considering the small number of observers) attest to their regular presence. The presence of a Red-necked Phalarope population off the coast of East Africa is further confirmed by regular reports from deep sea sports anglers of 'dozens of phalaropes' on the water and around the boat. Considering the difficulty of observing birds offshore (i.e. requiring observers to be at sea or in possession of a telescope) and the low observation pressure of seabirds in East Africa, it is likely that their presence and abundance along the Kenyan coast is largely under appreciated.

Impact of the 2019–2020 IOD on regional Red-necked Phalarope population

We suggest that the exceptionally high numbers of Red-necked Phalaropes observed in February 2020, were due to the extreme positive IOD event recorded in autumn 2019 in the following way. In regular years, some Red-necked Phalaropes move to the East African coast in the second part of their winter (January–February) benefiting from the usual upwelling forming in this region at this time of year (Figure 1a). However, in 2020, due to the extreme positive IOD and subsequent reduced upwelling (Figure 1b), they did not find their usual food and therefore resorted to moving closer to the coast, often at river estuaries (i.e. Kongo, Mida Creek, Sabaki, Tana Delta) where food is more readily available (Rubega et al. 2020).

This explanation is in line with the current understanding of Red-necked Phalaropes' movements in the region. Indeed, the timing of our sightings on the Kenyan coast (i.e. February) corresponds to the peaks (1) in NPP (Lévy et al. 2007), (2) in coastal sightings (Figure 3) and (3) of when tracked birds reach the coast of Kenya (Van Bemmelen et al. 2016, 2019). Their presence in East Africa despite the absence of NPP is consistent with the itinerancy hypothesis that their wintering movements are repetitive and consistent Van Bemmelen et al. (2019). This explanation also echoes the observed impact of the severe *El Niño* event that took place in the Pacific Ocean in 1982–1983, when the resulting drop in phytoplankton was held responsible for the high mortality of the Nearctic Red-necked Phalarope breeding population (Barber and Chavez 1983; Jehl Jr. 1986) and the subsequent crash of the Fundy Bay population (Duncan 1995; Nisbet and Veit 2015).

We did not find evidence for a linear relationship between the number of observations of Red-necked Phalaropes on the coast and the strength of IOD or NPP offshore (Figure 4, Figure 5, Figure A1 and Table A1 in Appendix A). Several reasons can explain the absence of relationship. Firstly, there is no reason to assume that the movement of Phalaropes towards the coast is linearly linked to the quantity of food. Rather, they might be pushed to the coast only when NPP reaches a certain threshold. Secondly, the strong heterogeneity in presence and expertise of observers on the coast renders the analysis unreliable. However, the 2020 record remains exceptional in light of the regular presence and monitoring by the A Rocha Kenya science team in the region since 2000 (Nussbaumer et al. 2021).

Red-necked Phalaropes might uniquely adapt to the absence of food offshore by coming near the coast because of their specific nature of wader displaying the wintering behaviour of a seabird. This behaviour might therefore not be generalisable to all seabirds. During the *El Niño* event of 1926, (Murphy 1936) reported large numbers of Red-necked Phalaropes off the coast of Peru, which might have been exhibiting a similar behaviour.

Implications for seabirds

Our investigation highlights the need to account for multiannual extreme events in our understanding of the strategy and evolution of seabird movements (e.g. Cubaynes et al. 2011). Indeed, such extreme events could potentially have wide consequences for the survival of seabird populations, as was the case for the extreme *El Niño of 1982–1983* (Barber and Chavez 1983; Jehl Jr. 1986; Veit et al. 1996). Systematic longer-term data on seabird abundance and distribution is required to analyse the impact of these extreme events characterised by decadal variability (Han et al. 2014).

Considering the likely reduction of NPP in the future (Roxy et al. 2016) and the increased occurrence of extreme IOD events since 2000 (Abram et al. 2008), which are expected to become even more frequent because of climate change (Cai et al. 2018), it is urgent we investigate in more detail the impact of extreme IOD events and of other such extreme weather events on seabirds in the Indian Ocean.

Acknowledgements — We thank Kirao Lennox, Mustafa Adamjee and Doris Schaule for organising and leading the 2020 waterbird counts.

Data Accessibility — All data (https://github.com/A-Rocha-Kenya/Red-Necked-Phalaropes-in-East-Africa/blob/main/R_code/sightings.csv) and code (https://a-rocha-kenya.github.io/Red-Necked-Phalaropes-in-East-Africa/R_code/Red-necked_Phalarope_publication.html) used in this research are available on open-access repository on Github (https://a-rocha-kenya.github.io/Red-Necked-Phalaropes-in-East-Africa/). The interactive and comparative map of NPP can be found at (https://rafnuss.users.earthengine.app/view/net-primary-productivity).

ORCIDs

Raphaël Nussbaumer: https://orcid.org/0000-0002-8185-1020
Mathieu Gravey: https://orcid.org/0000-0002-0871-1507
Améline Nussbaumer: https://orcid.org/0000-0003-1308-4154
Colin Jackson: https://orcid.org/0000-0003-2280-1397

References

Abram NJ, Gagan MK, Cole JE, Hantoro WS, Mudelsee M. 2008. Recent intensification of tropical climate variability in the Indian Ocean. *Nature Geoscience* 1: 849–853. https://doi.org/10.1038/ngeo357.

Ainley DG, Carter HR, Anderson DW, Briggs KT, Coulter MC, Cruz F, Cruz JB, Valle CA, Fefer SI, Hatch SA, et al. 1988. Effects of the 1982-83 *El Niño*--Southern Oscillation on Pacific Ocean bird populations. (pp 1747–1758). *19th International Ornithological Conference*. Ottawa: University of Ottawa Press. https://pubs.er.usgs.gov/publication/70189788.

Ash JS, Ashford OM. 1977. Great Black-headed Gulls *Larus ichthyaetus* and Red-necked Phalaropes *Phalaropus lobatus* inland in Ethiopia. *Journal of the East Africa Natural History Society and National Museum* 31: 1–3.

Ash JS, Miskell JE. 1998. *Birds of Somalia*. Bloomsbury Publishing.

Bailey R. 1966. The sea-birds of the southeast coast of Arabia. *Ibis* 108: 224–264. https://doi.org/10.1111/j.1474-919X.1966.tb07269.x.

Bailey RS. 1971. Sea-bird observations off Somalia. *Ibis* 113: 29–41. https://doi.org/10.1111/j.1474-919X.1971.tb05121.x.

Baker NE. 2013. Recent unprecedented numbers of Red-necked Phalaropes *Phalaropus lobatus* in Tanzania, and some older undocumented records. *Scopus* 32: 41–42.

Barber RT, Chavez FP. 1983. Biological consequences of *El Niño*. *Science* 222: 1203–1210. https://doi.org/10.1126/science.222.4629.1203.

Behera SK, Luo JJ, Masson S, Delecluse P, Gualdi S, Navarra A, Yamagata T. 2005. Paramount impact of the Indian Ocean Dipole on the East African short rains: A CGCM study. [American Meteorological Society]. *Journal of Climate* 18: 4514–4530. https://doi.org/10.1175/JCLI3541.1.

Behrenfeld MJ, Falkowski PG. 1997. Photosynthetic rates derived from satellite-based chlorophyll concentration. *Limnology and Oceanography* 42: 1–20. https://doi.org/10.4319/lo.1997.42.1.0001.

BirdLife International. 2020. Species factsheet: *Phalaropus lobatus*. http://datazone.birdlife.org/species/factsheet/22693490.

Bjerknes J. 1969. Atmospheric teleconnections from the equatorial pacific. *Monthly Weather Review* 97: 163–172. https://doi.org/10.1175/1520-0493(1969)097<0163:ATFTEP>2.3.CO;2.

Bost CA, Cotté C, Bailleul F, Cherel Y, Charrassin JB, Guinet C, Ainley DG, Weimerskirch H. 2009. The importance of oceanographic fronts to marine birds and mammals of the southern oceans. *Journal of Marine Systems* 78: 363–376. https://doi.org/10.1016/j.jmarsys.2008.11.022.

Britton PL. 1980. *Birds of East Africa: their habitat, status and distribution*. Nairobi: East Africa Natural History Society.

Britton PL, Britton HA. 1979. Phalaropes in Coastal Kenya. *Scopus* 3: 58.

Cai W, Wang G, Gan B, Wu L, Santoso A, Lin X, Chen Z, Jia F, Yamagata T. 2018. Stabilised frequency of extreme positive Indian Ocean Dipole under 1.5°C warming. *Nature Communications* 9: 4–11. https://doi.org/10.1038/s41467-018-03789-6.

Cai W, Zheng X, Weller E, Collins M, Cowan T, Lengaigne M, Yu W, Yamagata T. 2013. Projected response of the Indian Ocean Dipole to greenhouse warming. *Nature Geoscience* 6: 999–1007. https://doi.org/10.1038/ngeo2009.

Cubaynes S, Doherty PF, Schreiber EA, Gimenez O. 2011. To breed or not to breed: A seabird's response to extreme climatic events. *Biology Letters* 7: 303–306. https://doi.org/10.1098/rsbl.2010.0778.

Delany S, Scott D, Dodman T, Stroud D. 2009. *An atlas of wader populations in Africa and Western Eurasia*. Wageningen: Wetlands International.

Duncan C. 1995. The Migration of Red-necked Phalaropes: Ecological Mysteries and Conservation Concerns. *Bird Observer* 23: 200–208.

EBird. 2020. eBird: An online database of bird distribution and abundance [web application] http://www.ebird.org.

Franks PJS. 1992. Phytoplankton blooms at fronts: patterns, scales, and physical forcing mechanisms. *Reviews in Aquatic Sciences* 6: 121–137.

Gorelick N, Hancher M, Dixon M, Ilyushchenko S, Thau D, Moore R. 2017. *Google Earth Engine: Planetary-scale geospatial analysis for everyone.* Remote Sensing of Environment. Elsevier.

Han W, Vialard J, McPhaden MJ, Lee T, Masumoto Y, Feng M, De Ruijter WPM. 2014. Indian ocean decadal variability: A review. *Bulletin of the American Meteorological Society* 95: 1679–1703. https://doi.org/10.1175/BAMS-D-13-00028.1.

Heip CHR, Hemminga MA, Bie MJM. 1995. *Monsoons and coastal ecosystems in Kenya.* National museum of Natural History Leiden.

Hunt GL, Mehlum F, Russell RW, Irons D, Decker MB, Becker PH. 1999. Physical processes, prey abundance, and the foraging ecology of seabirds. (pp 2040–2056). In: Adams NJ, Slotow RH (Eds). *Proceedings of the 22nd International Ornithological Congress, Durban*. Johannesburg: BirdLife South Africa.

Hušek J, AdamÍk P, Cepák J, Tryjanowski P. 2009. The influence of climate and population size on the distribution of breeding dates in the Red-backed Shrike (*Lanius collurio*). *Annales Zoologici Fennici* 46: 439–450. https://doi.org/10.5735/086.046.0605.

Jacobs ZL, Jebri F, Raitsos DE, Popova E, Srokosz M, Painter SC, Nencioli F, Roberts M, Kamau J, Palmer M, et al. 2020a. Shelf-break upwelling and productivity over the north Kenya banks: the importance of large-scale ocean dynamics. *Journal of Geophysical Research: Oceans* 125: 1–18. https://doi.org/10.1029/2019JC015519.

Jacobs ZL, Jebri F, Srokosz M, Raitsos DE, Painter SC, Nencioli F, Osuka K, Samoilys M, Sauer W, Roberts M, et al. 2020b. A major ecosystem shift in coastal east African waters during the 1997/98 Super *El Niño* as detected using remote sensing data. *Remote Sensing* 12: 3127. https://doi.org/10.3390/rs12193127.

Jebri F, Jacobs ZL, Raitsos DE, Srokosz M, Painter SC, Kelly S, Roberts MJ, Scott L, Taylor SFW, Palmer M, et al. 2020. Interannual monsoon wind variability as a key driver of East African small pelagic fisheries. *Scientific Reports* 10: 1–15. https://doi.org/10.1038/s41598-020-70275-9.

Jehl Jr. JR. 1986. Biology of Red-necked Phalaropes (*Phalaropus lobatus*) at the western edge of the Great Basin in fall migration. *Great Basin Naturalist* 46: 185–197.

Kenya Bird Map. 2020. Kenya Bird Map. http://kenyabirdmap.adu.org.za.

Lévy M, Shankar D, André JM, Shenoi SSC, Durand F, De Boyer Montégut C. 2007. Basin-wide seasonal evolution of the Indian Ocean's phytoplankton blooms. *Journal of Geophysical Research: Oceans* 112: Issue C12.

Lewis A, Pomeroy D. 1989. *A Bird Atlas of Kenya*. Balkema AA (Ed.). Rotterdam: CRC Press. https://www.taylorfrancis.com/books/mono/10.1201/9781315136264/bird-atlas-kenya-adrian-lewis-derek-pomeroy.

Lu B, Ren HL. 2020. What caused the extreme Indian Ocean dipole event in 2019? *Geophysical Research Letters* 47: e2020GL087768. https://doi.org/10.1029/2020GL087768.

Marchant R, Mumbi C, Behera S, Yamagata T. 2007. The Indian Ocean dipole - the unsung driver of climatic variability in East Africa. *African Journal of Ecology* 45: 4–16. https://doi.org/10.1111/j.1365-2028.2006.00707.x.

Marsac F, Blanc J. 1999. Oceanographic changes during the 1997-1998 *El Niño* in the Indian Ocean and their impact on the purse seine fishery. *IOTC Proceedings no. 2*: 147–157. https://www.researchgate.net/publication/228694431_Oceanographic_changes_during_the_1997-1998_El_Nino_in_the_Indian_Ocean_and_their_impact_on_the_purse_seine_fishery. [Accessed 12 November 2021].

Monticelli D, Ramos JA, Quartly GD. 2007. Effects of annual changes in primary productivity and ocean indices on breeding performance of tropical roseate terns in the western Indian Ocean. *Marine Ecology Progress Series* 351: 273–286. https://doi.org/10.3354/meps07119.

Moreau RE. 1972. *Palaearctic-African bird migration systems*. New York: Academic Press.

Murphy RC. 1936. *Oceanic birds of South America*. New York: MacMillan Company.

Nisbet ICT, Veit RR. 2015. An explanation for the population crash of Red-necked Phalaropes *Phalaropus lobatus* staging in the Bay of Fundy in the 1980s. *Marine Ornithology* 43: 119–121.

Nussbaumer R, Lennox K, Baya A, Gijsbertsen J, Kinzer A, Jackson CHW. 2021. Waterbird counts at Sabaki River mouth and Mida Creek. Kenya: A Rocha. https://doi.org/10.15468/9hs9vv.

Nussbaumer R, Lennox K, Jackson C. 2020. National Waterbird Counts Report Kenya, Coast. http://doi.org/10.13140/RG.2.2.36630.57925. [Accessed 12 November 2021].

O'Malley R. 2020. Ocean Productivity. http://sites.science.oregonstate.edu/ocean.productivity. [Accessed 12 November 2021].

Painter SC. 2020. The biogeochemistry and oceanography of the East African Coastal Current. *Progress in Oceanography* 186: 102374. https://doi.org/10.1016/j.pocean.2020.102374.

Perez-Correa J, Carr P, Meeuwig JJ, Koldewey HJ, Letessier TB. 2020. Climate oscillation and the invasion of alien species influence the oceanic distribution of seabirds. *Ecology and Evolution* 10: 9339–9357. https://doi.org/10.1002/ece3.6621.

Pocklington R. 1979. An oceanographic interpretation of seabird distributions in the Indian Ocean. *Marine Biology* 51: 9–21. https://doi.org/10.1007/BF00389026.

Remisiewicz M, Underhill LG. 2020. Climatic variation in Africa and Europe has combined effects on timing of spring migration in a long-distance migrant Willow Warbler *Phylloscopus trochilus*. *PeerJ* 8: 1–30. https://doi.org/10.7717/peerj.8770.

Rivalan P, Barbraud C, Inchausti P, Weimerskirch H. 2010. Combined impacts of longline fisheries and climate on the persistence of the Amsterdam Albatross *Diomedia amsterdamensis*. *Ibis* 152: 6–18. e8770

Roxy MK, Modi A, Murtugudde R, Valsala V, Panickal S, Prasanna Kumar S, Ravichandran M, Vichi M, Lévy M. 2016. A reduction in marine primary productivity driven by rapid warming over the tropical Indian Ocean. *Geophysical Research Letters* 43: 826–833. https://doi.org/10.1002/2015GL066979.

Rubega MA, Schamel D, Tracy DM. 2020. Red-necked Phalarope (*Phalaropus lobatus*). In: Billerman SM (Ed.). *Birds of the World*. Cornell Lab of Ornithology, Ithaca, NY, USA. Retrieved from Birds of the World: https://birdsoftheworld.org/bow/species/renpha/1.0.

Saji N, Goswami B, Vinayachandran P, Yamagata T. 1999. A dipole mode in the Tropical Indian Ocean. *Nature* 401: 360–363. https://doi.org/10.1038/43854.

Schiemann H. 1986. Red-necked Phalaropes *Phalaropus lobatus* off the coast of Somalia and Kenya. *Scopus* 10: 42–44.

Schott FA, Xie SP, McCreary JP. 2009. Indian ocean circulation and climate variability. *Reviews of Geophysics* 47: 1–46. https://doi.org/10.1029/2007RG000245.

Shi W, Wang M. 2021. A biological Indian Ocean dipole event in 2019. *Scientific Reports* 11: 1–8.

Tobolka M, Dylewski L, Wozna JT, Zolnierowicz KM. 2018. How weather conditions in non-breeding and breeding grounds affect the phenology and breeding abilities of White Storks. *The Science of the Total Environment* 636: 512–518. https://doi.org/10.1016/j.scitotenv.2018.04.253.

Tøttrup AP, Klaassen RHG, Kristensen MW, Strandberg R, Vardanis Y, Lindström Å, Rahbek C, Alerstam T, Thorup K. 2012. Drought in Africa caused delayed arrival of European songbirds. *Science* 338: 1307. https://doi.org/10.1126/science.1227548.

Tryjanowski P, Stenseth NC, Matysioková B. 2013. The Indian Ocean Dipole as an indicator of climatic conditions affecting European birds. *Climate Research* 57: 45–49. https://doi.org/10.3354/cr01162.

Urban EK, Fry CH, Keith S. 1986. The birds of Africa. Vol. 2. London & New York: Academic Press.

Van Bemmelen RSA, Hungar J, Tulp I, Klaassen RHG. 2016. First geolocator tracks of Swedish Red-necked Phalaropes reveal the Scandinavia-Arabian Sea connection. *Journal of Avian Biology* 47: 295–303. https://doi.org/10.1111/jav.00807.

Van Bemmelen RSA, Kolbeinsson Y, Ramos R, Gilg O, Alves JA, Smith M, Schekkerman H, Lehikoinen A, Petersen IK, Pórisson B, et al. 2019. A migratory divide among Red-necked Phalaropes in the Western Palearctic reveals contrasting migration and wintering movement strategies. *Frontiers in Ecology and Evolution* 7: 1–17. https://doi.org/10.3389/fevo.2019.00086.

Veit R, Pyle P, McGowan J. 1996. Ocean warming and long-term change in pelagic bird abundance within the California current system. *Marine Ecology Progress Series* 139: 11–18. https://doi.org/10.3354/meps139011.

Vinayachandran PNM, Masumoto Y, Roberts M, Hugget J, Halo I, Chatterjee A, Amol P, Gupta GVM, Singh A, Mukherjee A, et al. 2021. Reviews and syntheses: Physical and biogeochemical processes associated with upwelling in the Indian Ocean. *Biogeosciences Discussions* 2021: 1–128.

Webster PJ, Moore AM, Loschnigg JP, Leben RR. 1999. Coupled oceanic-atmoshperic dynamics in the Indian Ocean during 1997-98. *Nature* 401: 356–360. https://doi.org/10.1038/43848.

Weimerskirch H. 2007. Are seabirds foraging for unpredictable resources? *Deep-Sea Research Part II: Topical Studies in Oceanography* 54: 211–223. https://doi.org/10.1016/j.dsr2.2006.11.013.

Wiggert JD, Vialard J, Behrenfeld MJ. 2009. Basin-wide modification of dynamical and biogeochemical processes by the positive phase of the Indian Ocean Dipole during the SeaWiFS era. In: *Indian Ocean Biogeochemical Processes and Ecological Variability.* Vol. 185. Washington, DC: American Geophysical Union (AGU). pp 385–407. https://agupubs.onlinelibrary.wiley.com/doi/abs/10.1029/2008GM000776.

Manuscript received: 17 April 2021, revised: 6 October 2021, accepted: 9 October 2021
Associate Editor: KN Oswald

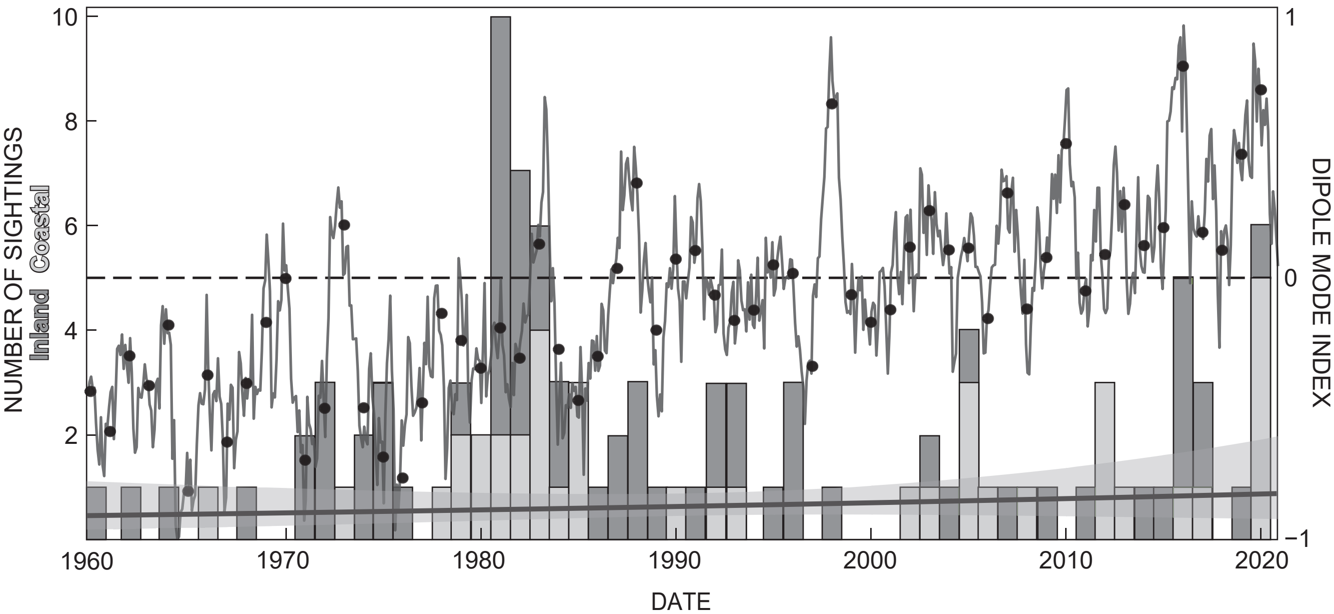

Figure A1: Number of sightings for each wintering period (October–March) on the coast (light grey) and inland (dark grey) together with the Dipole Mode Index timeseries for the same period (1960–2020). The average DMI for the wintering period is symbolised with a black dot. The partial plot of the fitted generalised linear model is illustrated with the solid grey line and corresponding uncertainty (grey area)

Table A1: Estimated regression parameters, standard errors, *z*-values and *p*-values for the Poisson GLM examining the relationship between net primary productivity (NPP) and dipole model index (DMI)

	Estimate	Standard error	*z*-value	*p*-value
		DMI ~ NPP		
(Intercept)	1.28	0.24	5.28	3.08 $\exp^{-0.05}$
NPP	−0.003	0.00057	−4.55	0.00017
		#sightings ~ DMI + year		
(Intercept)	−22.66	26.72	−0.85	0.34
DMI	0.47	0.63	0.74	0.46
Year	0.011	0.013	0.83	0.40